Oceanological and Hydrobiological Studies

International Journal of Oceanography and Hydrobiology

Volume 47, Issue 1, March 2018
pages (87-97)

ISSN 1730-413X
eISSN 1897-3191

Underwater noise emitted during small-scale air entrainment events

by

Justyna Szuszkiewicz[1,*],
Zygmunt Klusek[2]

DOI: **10.1515/ohs-2018-0010**
Category: **Short communication**
Received: **July 05, 2017**
Accepted: **September 29, 2017**

[1]*Department of Physical Oceanography, Institute of Oceanography, Faculty of Oceanography and Geography, Al. M. Piłsudskiego 46, 81-378 Gdynia, Poland*

[2]*Marine Acoustics Laboratory, Institute of Oceanology PAS, ul. Powstańców Warszawy 55, 81-712 Sopot, Poland*

Abstract

The breaking wave phenomenon significantly takes part in the mechanisms of mass, heat and gas exchange at the air-water boundary and depends on the wind velocity. Some of the energy dissipated during this process is converted into underwater sound emitted by oscillating gas bubbles and bubble plumes. However, the underwater noise accompanying the lowest wind speed conditions has received only little attention. This report describes a study aimed at advancing the knowledge of underwater noise emission from air bubbles injected during small-scale breaking events occurring on the water surface. Results of model experiments performed in a small tank are presented. The object of the research is the relationship between the generated noise and the dissipated potential energy of water poured into a tank filled with water of varying physical water properties. Additionally, the impact of various water properties such as salinity, surface tension or microscale gas bubbles was examined. The experiment revealed that noise spectra are affected by different water properties and most likely reflect the varying efficiency of bubble formation and bubble size spectra.

Key words: underwater noise, bubbles, bubble plumes, air entrainment

* Corresponding author: *justyna.szuszkiewicz@ug.edu.pl*

DE GRUYTER

The *Oceanological and Hydrobiological Studies* is online at oandhs.ocean.ug.edu.pl

Introduction

Mechanisms of underwater noise generation by natural sources in the sea is fairly well recognized. It was established that this noise is associated with the wave breaking process and is generated primarily after the injection of air bubbles below the water surface (Prosperetti 1988; Medwin & Beaky 1989; Medwin & Daniel 1990; Stagonas et al. 2011). Oscillations of both single bubbles and bubble plumes generate sound. This component of noise is wind-speed dependent and has a very broad spectrum that ranges from tens of Hz to tens of kHz. Single bubbles produce sound at frequencies above 1 kHz, while bubble plumes – at lower frequencies, generally below 500 Hz (Medwin & Daniel 1990; Kolaini et al. 1991; Loewen & Melville 1994; Orris & Nicolas 2000).

Underwater noise generated by breaking waves has often been studied and modeled under controlled conditions and all phases of its generation are well recognized (Medwin & Daniel 1990; Carey & Fitzgerald 1993; Nicholas et al. 1994; Means & Heitmeyer 2002; Klusek et al. 2013). The object of these studies is the relationship between underwater noise and surface wave energy, dissipated during breaking events. However, the breaking wave process was usually simulated by relatively energetic waves in a wave flume filled with tap water. Tęgowski (2004) and Deane & Stokes (2010) analyzed noise emitted during breaking waves with an amplitude of about 0.1 m, whereas Klusek & Lisimenka (2013) investigated single breakers with an amplitude exceeding 1.4 m.

Another class of simulation of underwater noise emission during wave breaking was carried out with the use of a tipping trough (Carey et al. 1993). It revealed differences in noise spectra between fresh and sea water, particularly in the high frequency range. Moreover, results of experiments performed in the wind channel in fresh and salt water also support this finding (Kolaini & Crum 1994; Kolaini 1998). Differences in sound spectra were interpreted as modifications of bubbles size spectra under the influence of ionic salt. In addition, differences between noise spectra produced by bubble clouds in the water of different salinity were accounted for bubble interactions inside the bubble plumes (Orris & Nicolas 2000).

It is well established that the linear relationship between the noise level and the logarithm of wind speed exists at winds above 5–6 m s^{-1}. However, noise emitted by sea surface appears below wind speed values of 4 m s^{-1}, when small-scale breaking and water splashes occasionally appear at the sea surface. Underwater noise produced by these small events received much less attention than their high energy counterparts. Consequently, we started our research to explain the influence of diverse physical water properties on the underwater sound generated during the smallest air entrainment events in controlled conditions. The experiment was performed in a small tank filled with water of varying salinity, surface tension and with the presence of gas microbubbles. In the last case, the observations performed in the presence of microbubbles corresponding to gas production in the sea by phytoplankton appear to be pioneering.

Materials and methods

Measurement scheme

Experiments were conducted in a small tank of 1.5 m length, 0.5 m width, 0.6 m height and filled with tap water to a depth of approximately 0.5 m. The water temperature was 19.5°C in the case of fresh water experiments and 20°C for saline water experiments. Additionally, a tipping trough of 3.8 l capacity was used to model small-scale air entrainment below the water surface. The tipping trough was attached to a height-adjusting rack with the possibility to control the potential energy of the water poured on the water surface. Four separated experiments were conducted to evaluate effects of different properties of water on the noise generation: fresh water, fresh water with surfactant, saline water, saline water with microbubbles (Table 1). Table 1 presents heights of the tipping trough (Table 1, column 1), for which a modeled event was carried out. The number of repetitions performed for each type of the water used in the experiment is presented in the successive columns of Table 1.

The surface tension of the water was lowered by adding a small amount of surfactant. The surfactant added to the water was a dish soap. The concentration

Table 1

The number of air entrainment events under different water conditions performed for particular heights of the tipping trough edge above the water surface

Tipping trough height above the water surface	Fresh water	Fresh water with surfactant	Saline water (8.5 PSU)	Saline water with microbubbles
0.02 m	9	-	7	8
0.03 m	9	7	7	7
0.04 m	-	6	7	7
0.05 m	9	6	9	8

of the dish soap added to the water was 1.1×10^{-5}. On the basis of data related to the main ingredients of the dish soap, the surface tension of the mixture should be between 2.5 and 3.5×10^{-2} N m^{-1}.

Salinity of 8.5 PSU was prepared from fresh water mixed with a proper amount of sea salt. The presence of a population consisting of small bubbles in the surface water layers in the sea was simulated through the process of electrolysis, powered by low-voltage DC (3V). Electrodes were made of three pairs of dental wires with a length of 0.27 m and spacing of 0.01 m.

Noise measurements and analysis

The acoustic signal was registered by four hydrophones HTI-96-MIN, mounted to vertical tubes with a controlled position of sensors. Hydrophones with built-in preamplifiers have a high sensitivity, i.e. about –170 dB re 1V µPa^{-1}. The frequency response of a hydrophone is linear in the range of 2 Hz–30 000 Hz and is estimated to cover the entire spectrum of underwater noise generated during the air entrainment modeling.

The experimental setup scheme is presented in Fig. 1. Hydrophones were placed at a depth of 0.15 m and positioned linearly along the center axis of the tank. The tipping trough was located at a distance of 0.9 m from the left side of the water tank. The distance from this wall to hydrophone 2 was 1.1 m, and to hydrophone 3 – 0.70 m. The interval between the hydrophones varied and was 0.19 m between transducers 1 and 2, and 0.24 m between transducers 3 and 4.

Along with recording of acoustic signals, a high resolution camera GoPro Hero 3 was employed to document the air injection events, evolution of bubble plumes and their depth entrainment.

Amplified signals were recorded using a ZOOM H6 recorder with a sampling frequency of 44.1 kHz or 96 kHz and with 16-bits resolution. The recorder sensitivity was calibrated with signals of known amplitude. Prior to sampling, an analog low-pass filter with a cut-off frequency of 20 kHz was used to prevent aliasing. Each waveform was analyzed for its pressure level as well as frequency composition.

Power Spectral Density (PSD) estimation was carried out using the FFT (Fast Fourier Transform) algorithm. In each case, the FFT was run on a subsequent time series, each with 1024 points. Calculations were made for all validated recordings. Data gathered for each case of the experiment, starting right before the water surface impact by the water flow (each 1.2 s long), were averaged. In addition, the noise spectral level (NSL) in one-third octave bands was computed.

Results

A high resolution camera allows for changes in the bubble plume generation and its evolution. Similarly to other experiments (Su et al. 1984; Deane & Stokes 2002), the sequence of events at first reveals a columnar bubble plume, which then transforms into a more diffuse cloud due to the turbulence motion and in the last phase, moves to the surface due to the buoyancy forces. Three examples of bubble clouds recorded by the camera at 0.05 m height of the tipping trough, one for each type of water, are shown in Fig. 2. Frequent deformations in spherical shape of the biggest bubbles can be observed there. Only small and medium size bubbles preserve their form. This reflects the situation when turbulence (pressure) in water deforms bigger bubbles as opposed to smaller ones, where the tension force plays a major role in maintaining the spherical shape. Larger bubbles usually reached the water surface faster than smaller ones (Detsch 1995; Leifer et al. 2000). However, their terminal velocity could be predicted in stagnant liquid only. Smaller bubbles were pushed deeper than those with a larger radius (Fig. 2).

The bubble plume formed after the air injection in various types of water resulted in evolution varying in time and extent (Fig. 2). Small-scale air entrainment events in fresh water resulted in smaller but compact bubble plumes that consisted mainly of bigger bubbles. A different experiment conducted in fresh water was the one with added surfactant. In

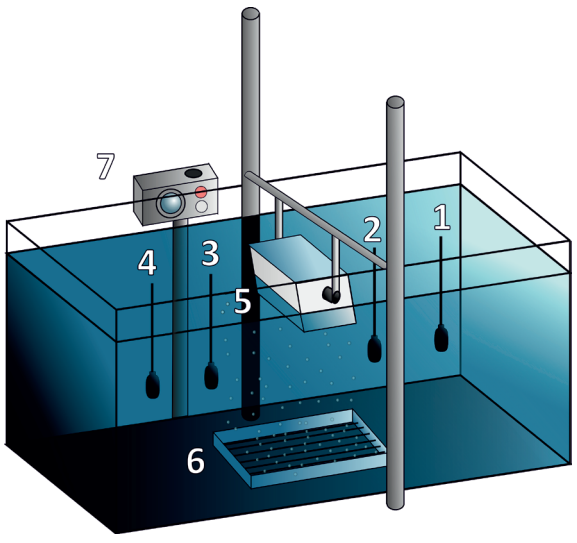

Figure 1

Scheme of the conducted experiment: 1, 2, 3, 4 – hydrophones, 5 – tipping trough used for wave generation, 6 – microbubbles generator, 7 – camera

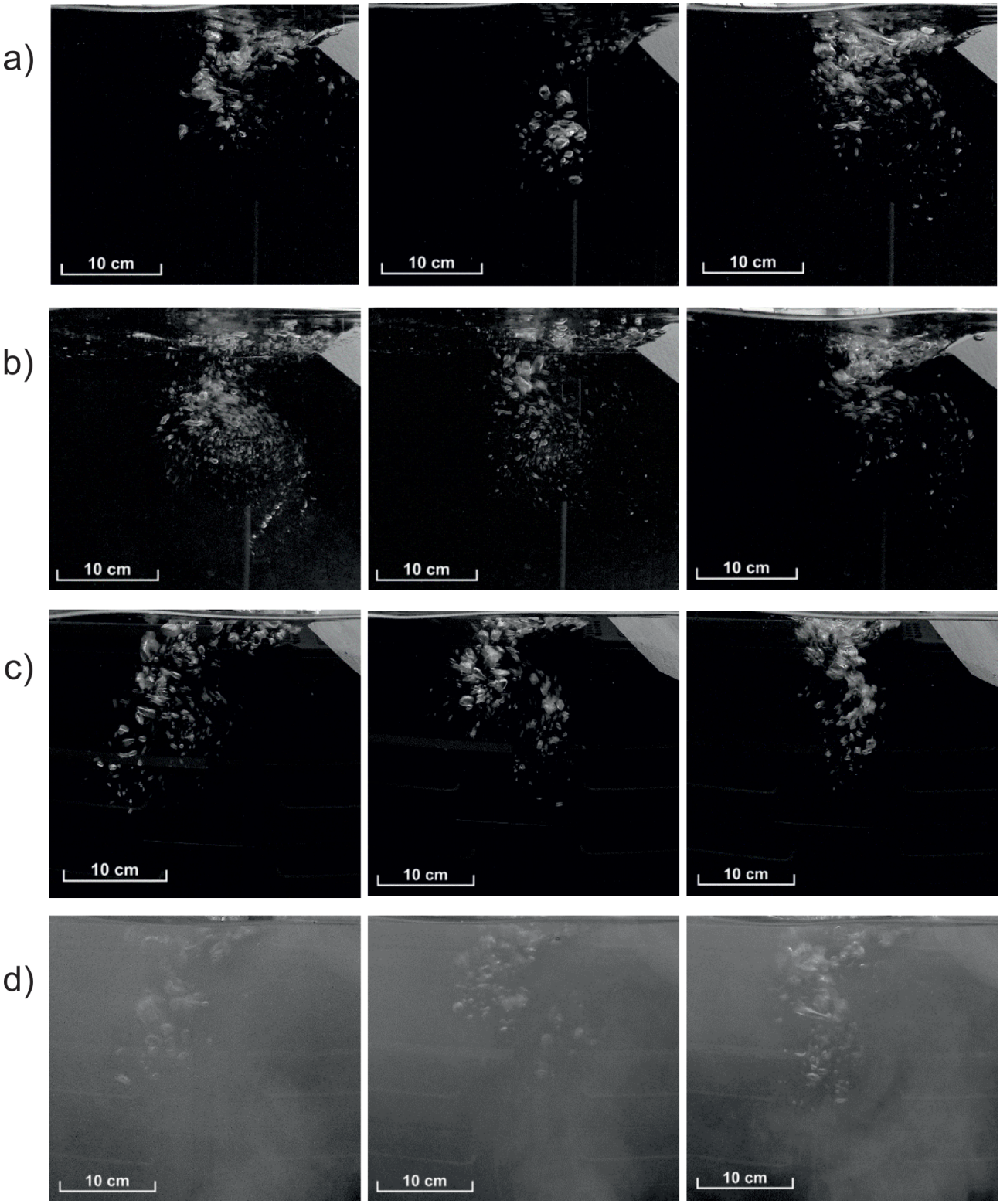

Figure 2

Comparison of the camera images of bubble plumes generated from 0.05 m of the tipping trough height for fresh water (a), fresh water with surfactant (b), saline water (c) and saline water with small bubbles (d)

comparison with the previous case, bubble plumes generated in these conditions were affected by stronger turbulent forces and penetrated deeper. According to Leifer et al. (2000), the presence of surfactant increases both the depth of the bubble entrainment and the subsequent duration of the degassing phase. It is supposed to be a result of the lower surface tension that allowed for the formation of smaller bubbles and more intensive aeration of the water. In this case, bubbles occurring on the surface after the degassing phase lasted longer than under other conditions and covered a large area.

The presence of microbubbles caused less dispersed character of bubble plumes consisting of bubbles with a smaller radius compared to fresh water. This was supported during experiments with electrolysis. The additional presence of tiny bubbles produced during electrolysis filled the entire bulk of the tank and, due to changes in compressibility of water, reduced the turbulence forces and further fragmentation of bubbles.

Every event generated a transient noise in water. An example of the pressure of the time series recorded by each of the four hydrophones during the air injection is shown in Fig. 3. The right side numbers correspond to the number of hydrophones presented in Fig. 1. Hydrophone 3 was located closest to the face edge of the bubble plume formed after the air entrainment, which resulted in the highest amplitude. As a consequence, there is a high possibility of flow noise occurrence (hydrodynamic disturbances or pseudo-sounds). Few cases of the modeled events were made toward the right part of the container. In these cases, hydrophone 2 was located closest to the breaker and was therefore excluded from the analysis of signals. The lowermost acoustic pressure was registered on hydrophone 1 due to the furthest location from the poured water and screening of a signal by bubbles. According to the above, hydrophone 4 characterized by the lowest hydrodynamic disturbances was selected for the presentation of the results.

One of the objectives of the preprocessing was to detect the starting point of the transient noise and to determine the window location on the time axis. Power spectral densities averaged over records of the repeated air entrainment, modeled from the same 0.05 m elevation of the tipping trough, are presented in the upper panel of Fig. 4. Furthermore, four examples of spectra obtained in separate air injection events are also shown below.

The comparison of the results for fresh and saline water revealed significant differences in the spectra shapes. The signal recorded in fresh water shows smaller values of PSD in the low frequency band. We observed strong fluctuations in the spectra, roughly above 3.5 kHz. Other differences include the presence of conspicuous peaks at the frequencies close to 2 kHz. This is most likely related to resonant frequencies in the tank (normal modes of oscillation in the tank).

The surfactant added to fresh water resulted in a higher spectrum level of the overall registrations. The most significant difference was observed in the low frequency range, from about 200 Hz. The estimated spectral slopes for both averaged fresh water cases were similar. In the frequency range up to 1 kHz, the spectral slope β was about $\beta \approx -4.5$ dB octave^{-1} and in the higher frequency area, it was $\beta \approx -9$ dB octave^{-1}.

Experiments carried out in saline water are characterized by a higher level of PSD in the low frequency range of the spectrum. The largest values are usually observed at frequencies around 200–300 Hz. Unlike the fresh water case, fluctuations of the signal in the high frequency range are relatively small. This phenomenon is evident in the spectra estimated in the presence of microbubbles, which was partly expected due to the fact that small bubbles substantially increase the sound attenuation in water. Spectral slopes calculated for saline water are more steep than in fresh water cases and are about −6 dB octave^{-1} in the low frequency range. There is a significant difference in the frequencies around 2 kHz, which also results from the geometry of the container. The noise spectrum level estimated for the case of the electrolysis more steeply declines toward higher frequencies and is about −15 dB octave^{-1}, while for saline water is −12 dB octave^{-1}.

The averaged spectrograms of the noise for each case of the experiment are given in Fig 5; only the situation of 0.05 m height of the tipping trough was

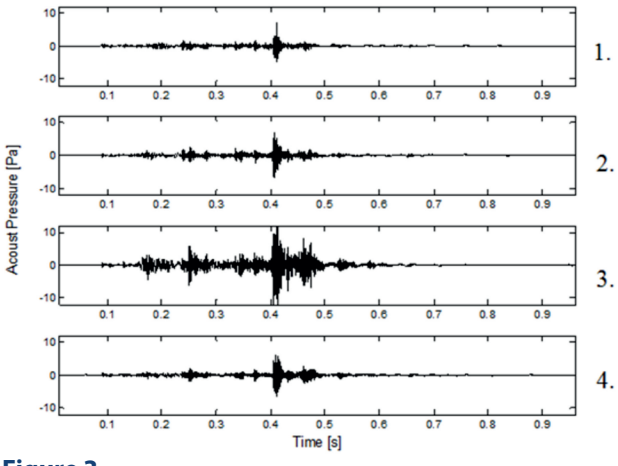

Figure 3

Time series of sound pressure recorded at four hydrophones. Numbering of hydrophones as in Fig. 1

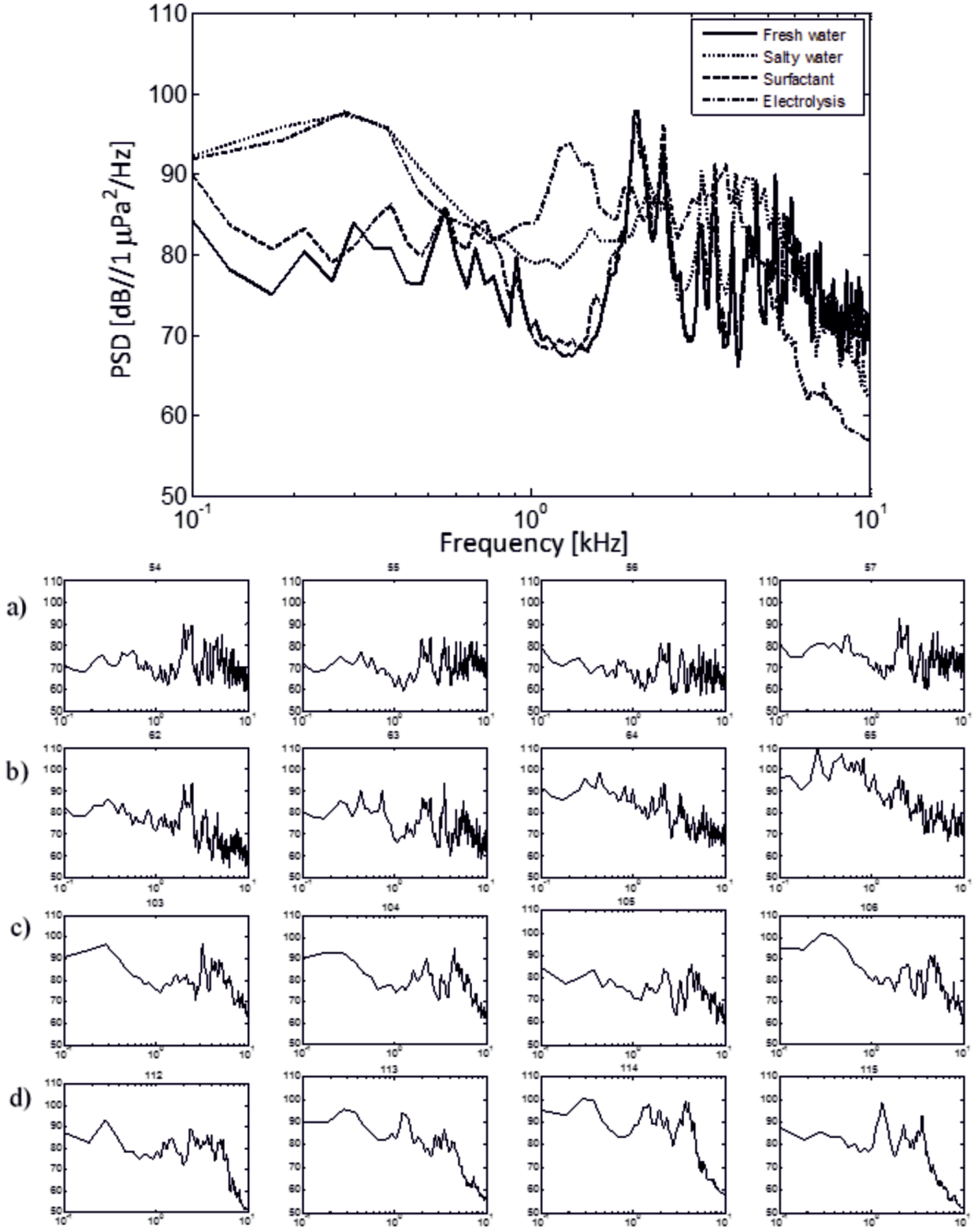

Figure 4

Averaged power spectra of underwater noise for each experiment case (upper part) with four examples of single events in fresh water (a), fresh water with surfactant (b), saline water (c), saline water with microbubbles (d) for 0.05 m height of the tipping trough

presented. Both spectrograms estimated for fresh water (clear and with surfactant) have a wide spectrum of frequencies related to underwater noise generated during the simulated air entrainment events. The highest values of power spectral density (PSD) were registered at approximately 2 kHz. The reduced surface tension allowed the release of a larger amount of energy in the low frequency range. In general, higher values of power spectral density were observed for modeled air injections in both saline water environments (saline water and the presence of microbubbles). The highest amount of energy of the emitted noise is limited to the lower frequency range: 6 kHz and 5 kHz, respectively. During the electrolysis process in the saline water, the damping effect becomes visible above 4 kHz. This situation was not observed in the fresh water conditions, where a broader range of frequencies was registered.

In addition to clear differences in the registered acoustic signal measured in various conditions, there is a relationship between the noise level and the potential energy of the tipping water volume (Fig. 6). Figure 6 shows the sound energy level (SEL) emitted from a single event as a function of the tipping trough elevation, recorded on each of the hydrophones for all given events and represents the whole amount of energy received at a particular location in the water for a given pulse. It was computed as an integral of the acoustic energy contained within the noise emitted after the water was poured, and is expressed in dB re 1 μPa^2 s. At this point, the term sound energy E_s is used in the generalized sense of signal processing as follows:

$$E_s = \int_0^{\tau} p^2(t)\, dt$$

where τ is the time between the splash of water poured onto the surface and the surface disturbance reflected from the tank wall. There is a clear positive tendency of acoustic energy in relation to the potential energy of tipping water volume. The highest values

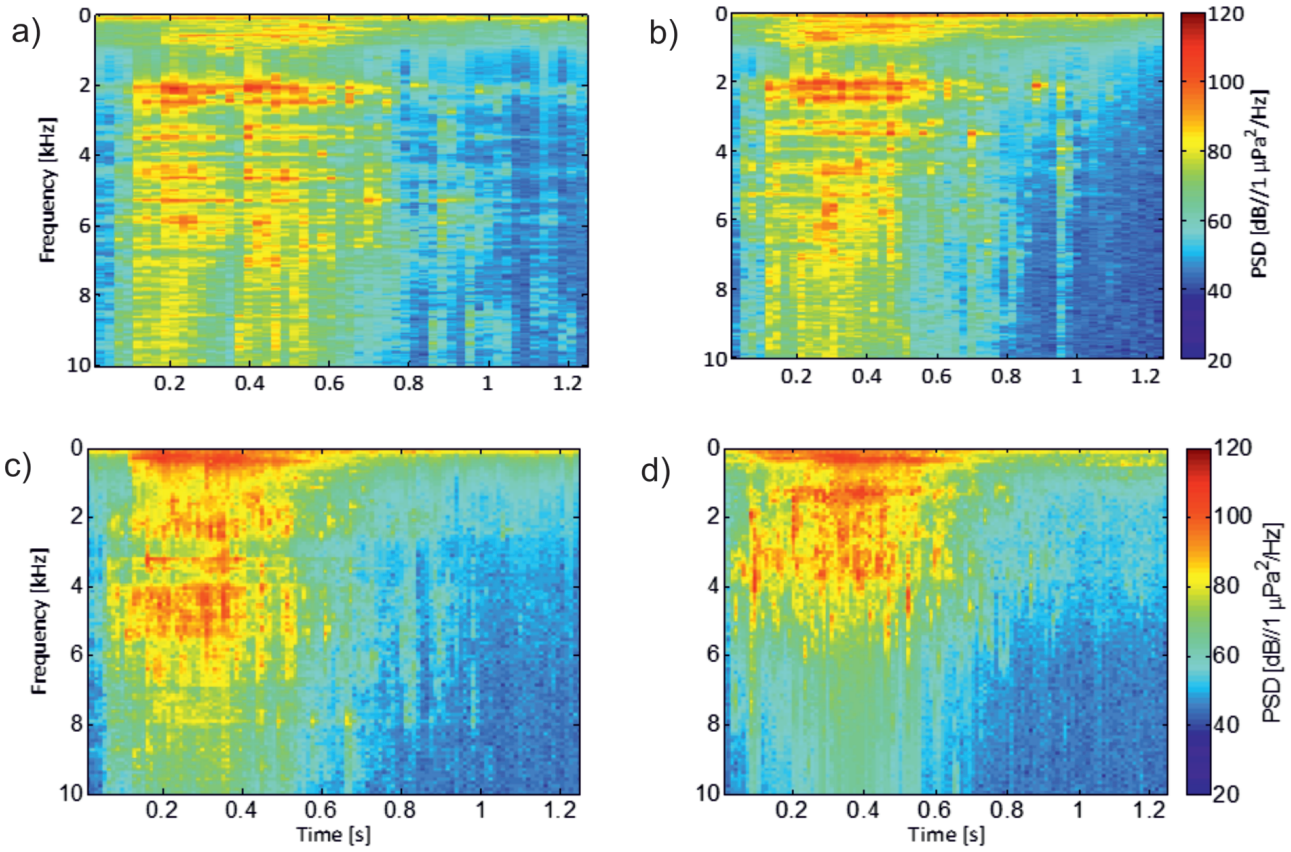

Figure 5

Spectrograms of averaged noise registered for 0.05 m height of the tipping trough in fresh water (a), water with surfactant (b), saline water (c) and water during the electrolysis process (d)

of acoustic energy are observed in the saline water situation. For the case with microbubbles, we assume that the smallest difference between the energy emitted at a height of 5 cm and 2 cm of the tipping trough was caused by highly attenuating environment.

Discussion and recommendations

The aim of this experiment was to determine the influence of various conditions on the acoustic energy produced during the simulation of the air entrainment events and to identify some trends accompanying this process. The underwater noise generation process during wave breaking is very complex and associated with environmental characteristics and water physico-chemical properties (Carey et al. 1993; Su & Cartmill 1995; Kolaini 1998; Orris & Nicolas 2000; Liu & Duncan 2003; Winkel et al. 2004).

The air injection events were simulated at various elevations of the tipping trough and different amounts of energy were released during specific processes. The two types of water, i.e. fresh and saline water, are shown in Fig. 7 along with the noise spectral level (NSL) calculated in one-third octave bands.

There is a clear positive relationship between the acoustic energy and the height of the water volume. This phenomenon is related to the potential energy of the water mass in the tipping trough. Subsequently, kinetic energy of the poured water, further associated with the intensity of produced gas bubbles pushed into the water body, resulted in the generation of high acoustic noise. The low-frequency area reveals a significant difference in the amount of generated acoustic energy. We suppose that this situation is a consequence of collective oscillations of the bubble clouds formed in saline water. Similar observations were reported by Yoon & Choi (1994) as well as by Kolaini (1998) who observed the same phenomenon.

A similar comparison was made for both types of saline water: saline water and saline water with the presence of microbubbles (Fig. 8). The same positive relationship was observed but, in contrast to the previous comparison, the most significant difference

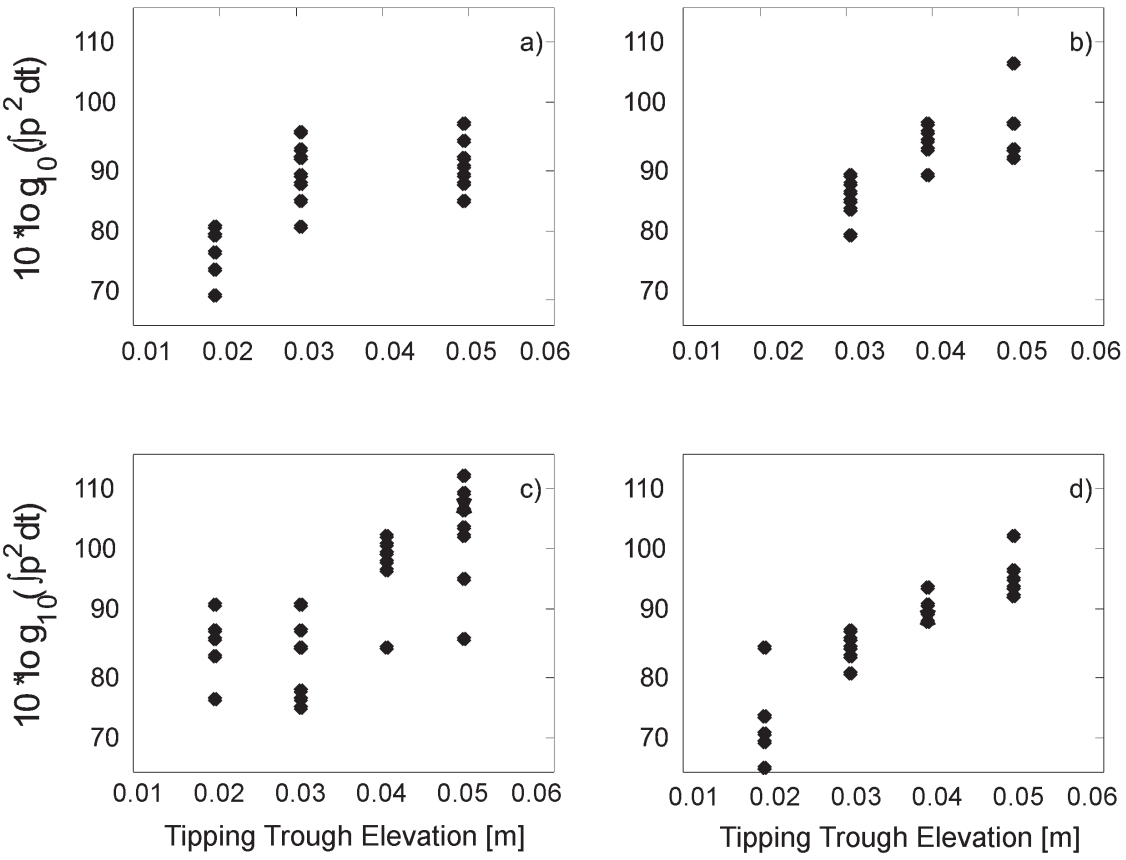

Figure 6

Total acoustic energy registered from a single air entrainment event as a function of the tipping trough elevation for fresh water (1), water with surfactant (2), saline water (3) and water during the electrolysis process (4)

was recorded in the high frequency range. The energy of the signal during the electrolysis process is reduced, which could be caused by a highly dumping environment of the medium filled with small bubbles. Furthermore, under registrations in saline water, hydrophones were covered by tiny bubbles. The highest concentration of a bubble film was observed during the electrolysis process. This could lead to some uncertainty of the registrations and could affect the hydroacoustic signal that reached a transducer. This situation did not occur on such a scale during measurements in fresh water.

The results of the conducted experiment are to some extent incomplete and distorted due to the geometry of the tank. Its small size affects the observed spectra and their level due to the phenomenon of standing wave (the result of multiple waves reflected from glass walls). The resonant frequencies f_{res} in a rectangular glass tank with dimensions L_x, L_y, L_z would be approximated by the formula (Akamatsu et al. 2002; Leighton et al. 2002):

$$f_{res} = \frac{c}{2}\sqrt{\left(\frac{l}{L_x}^2\right) + \left(\frac{m}{L_y}^2\right) + \left(\frac{n}{L_z}^2\right)}$$

where l, m, n = 1, 2, 3, … represent an integer number corresponding to the mode numbers, and the lowest mode number can be expressed as (1, 1, 1). Resonant frequencies also depend on the speed of sound in the medium c, which in turn depends on temperature and salinity. The experiments were conducted at a constant temperature; only salinity varied. The speed of sound estimated for fresh water was 1482 m s^{-1} and for saline water – by 10 m s^{-1} higher. When comparing the calculations for fresh and saline water, the resonant frequencies had very similar values. For the tank used in the experiment, the first mode was estimated at approximately 2.1 kHz. The resonant frequencies of the first three modes in saline water are shown in Fig. 9. Both x and z axes correspond to the mode number, but the resonant frequency is presented in the vertical axis.

A similar experiment, however at a different scale, was carried out by Carey et al. (1993) in lake and salt water. A tipping trough was also used in that experiment, but water was discharged from greater heights, resulting in a larger amount of released energy. The noise spectra in the case of fresh water were lower than those for salt water. Furthermore, a major low-frequency spectral peak near 100 Hz was observed for both types of water. For frequencies over 4 kHz, the noise spectrum level in seawater exceeds the noise spectrum level in fresh water. The authors have attributed this phenomenon to the larger amount

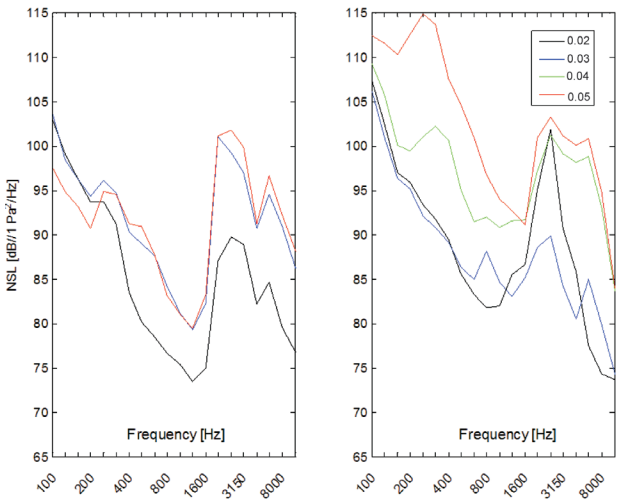

Figure 7

Comparison of averaged NSL in third-octave bands for 0.02, 0.03, 0.04 and 0.05 m height of the tipping trough for fresh water (a) and saline water (b)

of small bubbles generated in saline water. They found that averaged spectra, both in saline and fresh water, had the same spectral slope of approximately –12 dB octave^{-1} in the frequency range of 100 Hz–1 kHz. This value is similar to our results for the saline water type, but in the case of fresh water the spectral slope was less steep. The main reason for the differences between our results and those obtained by Carey et al. (1993) is that their experiment was

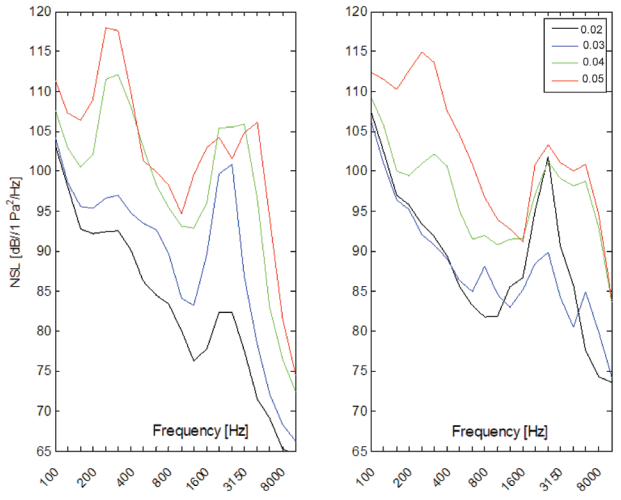

Figure 8

Comparison of averaged NSL in third-octave bands for 0.02, 0.03, 0.04 and 0.05 m height of the tipping trough for saline water (a) and during the electrolysis process in saline water (b)

conducted in situ on a larger scale, so the reverberation did not occur.

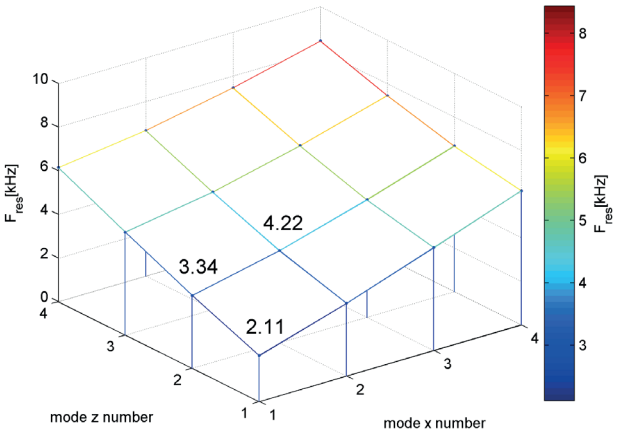

Figure 9

Resonant frequencies of the first three mixed modes in the tank

Summary

The study focuses on acoustic problems related to the potential impact of specific water properties on the noise generated during small-scale air entrainment events in the controlled conditions.

Camera registrations revealed differences in the process of formation of bubble plumes and their behavior. The most turbulent process occurred in fresh water with surfactant, and the least one in pure fresh water.

Every single case of the experiment produced different spectra of the underwater noise and proved that even small-scale water injections are strongly dependent of the environment. Both fresh water and fresh water with surfactant showed strong fluctuations of the noise level in the high frequency range. The added surfactant increased the level of low frequency noise compared to fresh water. The opposite situation was observed in both saline water experiments, where the highest underwater noise was registered in the low frequency range. We assume that this situation was caused by clusters of bubbles that oscillate as a whole. The electrolysis employed in the experiment simulated a persistent microbubble layer in the ocean produced by phytoplankton. It was observed that the presence of small bubbles, i.e. a high frequency component of the noise, was attenuated.

As expected, small-scale air entrainment events produce a small amount of acoustic energy. However, natural underwater noise produced over a large area should contribute to overall ambient noise. Sound energy of a single event is positively correlated with the elevation of the tipping trough. However, this relationship varied for all cases of the experiment.

Data on small air injections have been rarely reported in the literature, making it difficult to compare the noise data for different experiments. It should be emphasized that there is no common approach to the measurements made by different researchers, using a number of various methodologies.

References

Akamatsu, T., Okamura, T., Novarini, N. & Han, H.Y. (2002). Empirical refinements applicable to the recording of fish sounds in small tanks. *Journal of the Acoustical Society of America* 112(6): 3073–3082. DOI: 10.1121/1.1515799.

Carey, W.M. & Fitzgerald, J.W. (1993). Low frequency noise from breaking waves. In B.R. Kerman (Ed.) *Natural Physical Sources of Underwater Sound* (pp. 277–304). Springer Netherlands.

Carey, W.M., Fitzgerald, J.W., Monahan, E.C. & Wan, Q. (1993). Measurement of the sound produced by a tipping trough with fresh and salt water. *Journal of the Acoustical Society of America*. 93(6): 3178–3192. DOI: 10.1121/1.405702.

Deane, G.B. & Stokes, M.D. (2002). Scale dependence of bubble creation mechanisms in breaking waves. *Nature* 418: 839–844. DOI: 10.1038/nature00967.

Deane, G.B. & Stokes, M.D. (2010). Model calculations of the underwater noise of breaking waves and comparison with experiment. *Journal of the Acoustical Society of America* 127(6): 3394–3410. DOI: 10.1121/1.3419774.

Detsch, R.M. (1995). Small air bubbles in reagent grade water and seawater: 1. Rise velocities of 20- to 1000-μm-diameter bubbles. *Journal of Geophysical Research* 96: 8901–8906. DOI: 10.1029/91JC00484.

Han, L. & Yuan, Y. (2007). Bubble size distribution in surface wave breaking entraining process. *Science China Earth Sciences* 50(11): 1754–1760. DOI: 10.1007/s11430-007-0116-7.

Klusek, Z. & Lisimenka, A. (2013). Acoustic noise generation under plunging breaking waves. *Oceanologia* 55(4): 809–836. DOI: 10.5697/oc.55-4.809.

Klusek, Z., Dragan, A., Sulisz, W. & Dargacz, A. (2013). Dependence of acoustic noise generation on dissipation energy of plunging waves. In 1st International Conference and Exhibition on Underwater Acoustics, 23–26 June 2013 (pp. 951–956). Corfu, Greece.

Knudsen, V.O., Alford, R.S. & Emling, J.W. (1948). Underwater ambient noise. *Journal of Marine Research* 7: 410–429.

Kolaini, A.R., Roy, R.A. & Crum, L.A. (1991). An investigation of the acoustic emissions from a bubble plume. *Journal of the Acoustical Society of America*. 89(5): 2452–2455. DOI:

10.1121/1.400931.

Kolaini, A.R. & Crum, L.A. (1994). Observations of underwater sound from laboratory breaking waves and the implications concerning ambient noise in the ocean. *Journal of the Acoustical Society of America* 96(3): 1755–1765. DOI: 10.1121/1.410254.

Kolaini, A.R. (1998). Sound radiation by various types of laboratory breaking waves in fresh and salt water. *Journal of the Acoustical Society of America* 103(1): 300–308. DOI: 10.1121/1.421115.

Leifer, I., Patro, R.K. & Bowyer, P. (2000). A Study on the Temperature Variation of Rise Velocity for Large Clean Bubbles. *Journal of Atmospheric and Oceanic Technology* 17(10): 1392–1402. DOI: 10.1175/1520-0426(2000)017<1392:ASOTTV>2.0.CO;2.

Leighton, T.G., White, R.R., Morfey, C.L., Clarke, J.W., Heald, G.J. et al. (2002). The effect of reverberation on the damping of bubbles. *Journal of the Acoustical Society of America* 112(4): 1366–1376. DOI: 10.1121/1.1501895.

Liu, X., & Duncan, J.H. (2003). The effects of surfactants on spilling breaking waves. *Nature* 421: 520–523. DOI: 10.1038/nature01357.

Loewen, M.R. & Melville, W.K. (1994). An experimental investigation of the collective oscillations of bubble plumes entrained by breaking waves. *Journal of the Acoustical Society of America* 95(3)*:* 1329–1343. DOI: 10.1121/1.408573.

Means, S.C. & Heitmeyer, R.M. (2002). Surf-generated noise signatures: a comparison of plunging and spilling breakers. *Journal of the Acoustical Society of America* 112(2): 481–488. DOI: 10.1121/1.1491256.

Medwin, H. & Daniel, A.C. (1990). Acoustical measurements of bubble production by spilling breakers. *Journal of the Acoustical Society of America* 88(1): 408–4012. DOI: 10.1121/1.399917.

Nicholas, M., Roy, R.A., Crum, L.A., Oguz, H. & Prosperetti, A. (1994). Sound emissions by a laboratory bubble cloud. *Journal of the Acoustical Society of America* 95(6): 3171–3182. DOI: 10.1121/1.409981.

Orris, G.J. & Nicolas, M. (2000). Collective oscillations of fresh and salt water bubble plumes. *Journal of the Acoustical Society of America*. 107(2): 771–787. DOI: 10.1121/1.428253.

Stagonas, D., Warbrick, D., Muller, G. & Magagna, D. (2011). Surface tension effects on energy dissipation by small scale, experimental breaking waves. *Coastal Engineering* 58(9): 826–836. DOI: 10.1016/j.coastaleng.2011.05.009.

Su, M.-Y., Green, A.W. & Bergin, M.T. (1984). Experimental studies of surface wave breaking and air entrainment. In W. Brutsaert & G.H. Jirka (Eds.). *Gas transfer at water surfaces* (pp. 211–219). Dordrecht: Springer Netherlands.

Su, M.Y., & Cartmill, J. (1995). Effects of salinity on breaking wave generated void fraction and bubble size spectra. In Air-Water Gas Transfer, 24–27 July 1995 (pp. 305–311). Heidelberg University.

Tęgowski, J. (2004). A laboratory study of breaking waves. *Oceanologia* 46(3): 365–382.

Wenz, G.M. (1962). Acoustic ambient noise in the ocean: spectra and sources. *Journal of the Acoustical Society of America* 34(12): 1936–1956.

Winkel, E.S., Ceccio, S.L., Dowling, D.R. & Perlin, M. (2004). Bubble-size distributions produced by wall injection of air into flowing freshwater, saltwater and surfactant solutions. *Experiments in Fluids* 37(6): 802–810. DOI: 10.1007/s00348-004-0850-y.

Yoon, S.W. & Choi, B.K. (1994). Active and passive acoustic roles of bubbles in the ocean. In J.R. Blake, J.M. Boulton-Stone & N.H. Thomas (Eds.), *Bubble Dynamics and Interface Phenomena: Proceedings of an IUTAM Symposium Held in Birmingham, United Kingdom, 6–9 September 1993* (pp. 151–160). Dordrecht: Springer Netherlands.